Light: Science & Applications (2012) 1, e12; doi:10.1038/lsa.2012.12
© 2012 CIOMP. All rights reserved 2047-7538/12
www.nature.com/lsa

REVIEW

Bismuth-doped optical fibers: a challenging active medium for near-IR lasers and optical amplifiers

Evgeny M Dianov

It has recently been demonstrated that Bi-doped glass optical fibers are a promising active laser medium. Various types of Bi-doped optical fibers have been developed and used to construct Bi-doped fiber lasers and optical amplifiers. This paper reviews the recent results regarding the luminescence properties of various Bi-doped optical fibers and the development of Bi-doped fiber lasers and optical amplifiers for the 1150 to 1550 nm spectral region.
Light: Science & Applications (2012) **1,** e12; doi:10.1038/lsa.2012.12; published online 25 May 2012

Keywords: amplifier; bismuth; fiber; laser; luminescence

INTRODUCTION

Since the appearance of the first laser in 1960, significant attention has been devoted to the identification and the generation of new active laser media. This research made it possible to improve the characteristics of the existing lasers and to develop new ones. Active glass optical fibers are one of the most efficient laser media. Fiber lasers have excellent beam quality and are the most efficient solid-state lasers. Until recently, only rare earth-doped optical fibers have been used in the construction of fiber lasers and optical amplifiers.

At present, rare earth-doped fiber lasers with wavelengths in the near-IR region are widely used, including in optical communication, medicine, material processing and many other applications. However, within a spectral region of 1150–1500 nm, no efficient rare earth-doped fiber lasers exist. Because this spectral region could be used in advanced optical communication systems, in medicine and astrophysics and in other important applications, there is great demand for new active materials that are suitable for the creation of fiber lasers and optical amplifiers in this spectral region. Previous attempts to develop efficient transition metal-doped active materials have been unsuccessful.

In 2001, a paper that described broadband near-IR luminescence in Bi-doped silica-based glass was published.[1] Figure 1 shows the luminescence and transmission spectra of Bi-doped Al_2O_3–SiO_2 glass. The luminescence band at 1250 nm with a bandwidth of 300 nm is of significant interest, because it can be used in the construction of lasers and wideband optical amplifiers in the spectral region described above. The results have caused significant activity in the development of various Bi-doped glasses, in which strong broadband near-IR luminescence has been observed. A brief review of the first results indicating the luminescence properties of various Bi-doped glasses is presented in Ref. 2. In this paper, the luminescence spectra of several wide-spread Bi-doped glasses are shown in Figure 2. Figure 2a shows

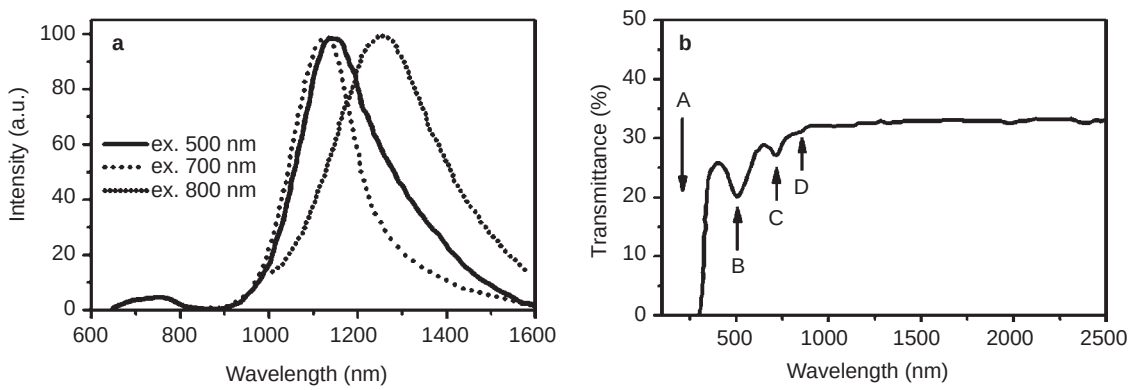

Figure 1 The luminescence (**a**) and transmission (**b**) spectra of Bi-doped aluminosilicate glass. The A, B, C, D arrows show the absorption bands of this glass. Excitation of luminescence at 500, 700 and 800 nm.

The Fiber Optics Research Center of the Russian Academy of Sciences, 119333 Moscow, Russia
Correspondence: Professor EM Dianov, The Fiber Optics Research Center of the Russian Academy of Sciences, 38 Vavilov str., 119333 Moscow, Russia
E-mail: dianov@fo.gpi.ru
Received 29 February 2012; revised 18 April 2012; accepted 21 April 2012

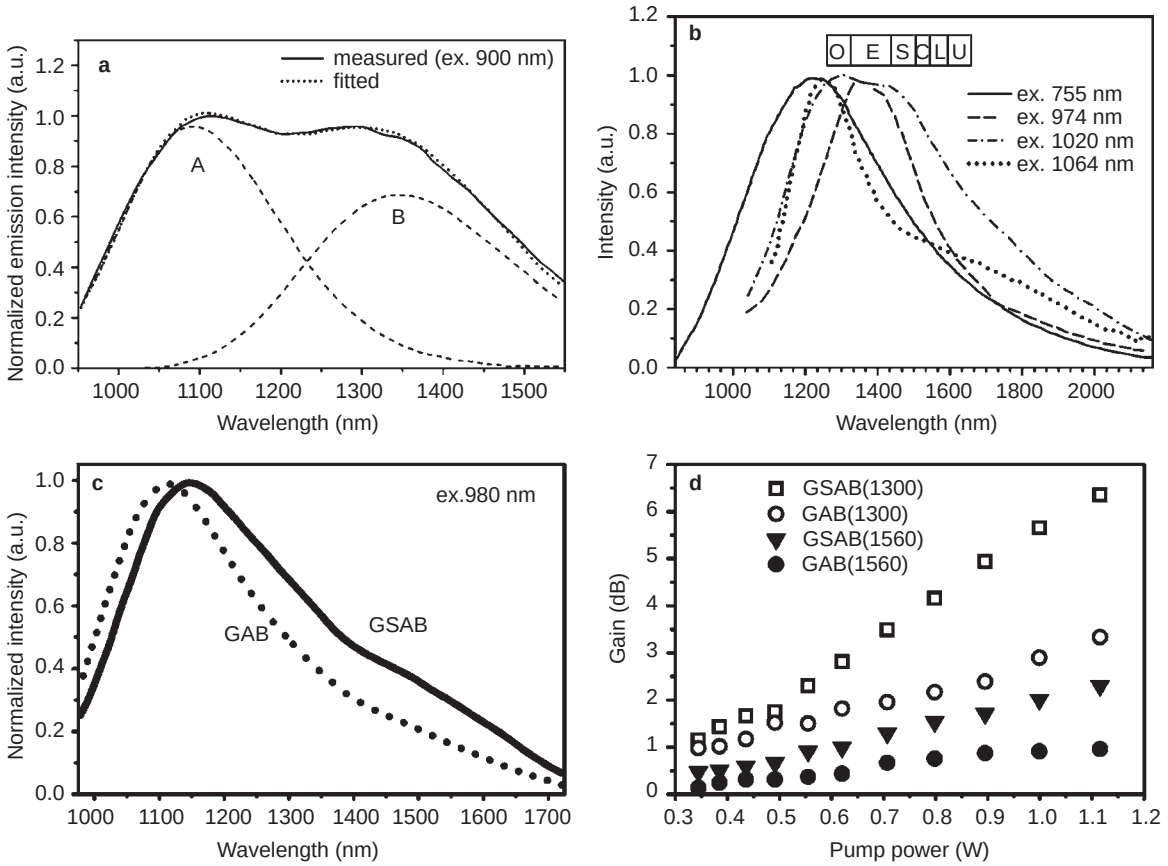

Figure 2 The luminescence spectra of Bi-doped Li_2O-Al_2O_3-SiO_2 glass (**a**), chalcogenide glass (**b**), germanate and germanium silica glasses (**c**) and internal gain at 1300 and 1560 nm as a function of pumping power (**d**). O,E,S,C,L,U, the standard telecommunication bands.

the luminescence spectrum of Bi-doped Li_2O–Al_2O_3–SiO_2 glass, as obtained by excitation at 900 nm.[3] Broadband luminescence (1000–1500 nm) was observed with two overlapping bands with maxima at 1100 and 1350 nm. The lifetime values for emissions at 1100 and 1350 nm are 549 and 270 μs, respectively.

Figure 2b shows the luminescence spectra of Bi-doped chalcogenide glass (gallium lanthanum sulfide) obtained at various pumping wavelengths.[4] As pictured, the luminescence of this glass extends to and exceeds 2000 nm.

Figure 2c shows the luminescence spectra of Bi-doped germanate (GAB) and germanium silicate (GSAB) glass containing 3 mol-% of aluminum oxide excited by 980-nm laser radiation.[5] The spectral region is 1000–1700 nm. The authors measured the gain dependence on the pump power at various wavelengths in 4-mm glass samples. The gain values of 5–6 dB at 1300 nm were obtained at 980 nm pump power ~1 W (Figure 2d).

Given the luminescence spectra of these Bi-doped glasses, it appears that Bi-doped glass may indeed be a promising active medium for near-IR lasers and optical amplifiers.

NATURE OF BI-RELATED NEAR-IR-EMITTING CENTERS

To date, the nature of Bi-related near-IR-emitting centers has been unclear, which has made it difficult to create efficient active laser media using Bi-doped glass. In fact, laser generation has not yet been possible using bulk Bi-doped glass. What are the problems that prevent one from understanding the nature of Bi-related near-IR-emitting centers?

Bismuth is a polyvalent element with four oxidation states: Bi^{5+}, Bi^{3+}, Bi^{2+} and Bi^{+}. Two processes take place in molten polyvalent element-doped glass: oxidation (at a higher valence state) and reduction (at a lower valence state).[6] The polyvalent ions in molten glass are in reduction/oxidation (redox) equilibrium, as described by the equation:

$$Me^{x+n} + \frac{n}{2}O^{2-} \rightleftarrows Me^{x} + \frac{n}{4}O_2$$

Me^{x+n} and Me^{x} are polyvalent ions in oxidation and reduction, respectively; n represents the number of transferred electrons.

These processes depend strongly on the melting temperature, glass composition, atmosphere and concentration of polyvalent elements. Usually, Bismuth oxide Bi_2O_3 (oxidation state 3+) is used as a raw material in Bi-doped glass synthesis. Generally, the redox equilibrium of metal ions moves toward the reduction side with increasing melting temperature. Bismuth is 'the wonder metal': with no other element do reduction reactions proceed so extensively and produce such a variety of products.[7] With increasing melting temperatures among Bi-doped glasses, the following change in the valence state of Bismuth takes place:[8]

$$Bi^{3+} \rightarrow Bi^{2+} \rightarrow Bi^{+} \rightarrow Bi \rightarrow \text{Bi clusters}$$

$$(\text{e.g., } Bi_2,\ Bi_2^{-}, Bi_3) : \rightarrow (Bi)_n \text{ colloids}$$

These features of Bi make it notably difficult to determine the valence state of Bi and therefore the exact nature of Bi-related near-IR-emitting centers in glass.

doi:10.1038/lsa.2012.12

However, there are two definite experimental facts:

- It is well-known that Bi^{3+} and Bi^{2+} ions emit visible luminescence and no near-IR luminescence.[9–12]
- The results of many experiments clearly demonstrate that near-IR luminescence is observed because of the reduction of Bi^{3+} ions to a lower oxidation state. Excessive reduction results in the formation of Bi clusters and colloids, and optical losses increase.[8,13]

At present, there are several hypotheses concerning the origin of near-IR emission from Bi-doped glass: Bi^{+}, Bi clusters, BiO, Bi_2^{-}/Bi_2, Bi_2^{-}/Bi_2^{2-}, point defects, Bi^0 and others have been examined, but none has been directly confirmed to be the defining factor. These hypotheses have been analyzed in detail in Ref. 14. At the same time, the results of extensive research on the luminescence spectra and lasing performance of crystals doped with Tl and Pb—bismuth's neighbors in the sixth period of the Periodic Table, which have similar properties—allow more definite conclusions to be drawn regarding the origin of near-IR Bi luminescence in glass and glass optical fibers.[15]

The optical properties of Tl-doped alkali halide crystals (KCl, KBr, RbCl and others) were studied extensively in the 1980s. X-ray and γ-irradiation was shown to produce near-IR-emitting defect centers in these materials (see, e.g., Refs. 16–19 and references therein). Detailed studies of such centers enabled the structure of at least three of them to be identified. The Tl^0 (1) and Tl^0 (2) centers take the form of a Tl^0 neutral atom on the cation site near an anion vacancy and between anion vacancies, respectively. Tl^0 (1) is a lasing center with transitions that enable laser operation tunable from 1400 to 1700 nm.[17,18] A Tl dimer center is composed of Tl^{+} and Tl^0 near an anion vacancy.[19] This center has three absorption bands in the 635–1110 nm range and emits in a range of 1450–1505 nm in KCl, RbCl and KBr crystals.

The X-ray irradiation of Pb-doped CaF_2, SrF_2 and BaF_2 crystals was reported to produce similar near-IR-emitting centers.[20,21] These centers include Pb^{+} (1) (a Pb^{+} ion near an anion vacancy), a Pb^{+} (1)–Pb^{2+} dimer (Pb^{+} and Pb^{2+} near a vacancy) and Pb^0 (2) (Pb^0 between two anion vacancies). The relative numbers of these centers depend on the irradiation temperature and initial Pb concentration. The formation of such optical centers is not accidental: Tl^0 and Tl^{+} are isoelectronic with Pb^{+} and Pb^{2+}, respectively. These centers have absorption bands within a range of 600–1100 nm and emit in a range of 1000–1700 nm in the crystal SrF_2.

Near-IR luminescence was also observed at 1070 and 1500 nm in Bi-doped BaF_2 crystal pumped at 500 and 700 nm [22]. Given that Bi^{2+} and Bi^{+} are isoelectronic with Pb^{+} and Pb, respectively, these luminescence bands were assigned to Bi^{2+} (1) and Bi^{+} (2) centers analogous to the Pb^{+} (1) and Pb^0 (2) centers.

Thus, at excitation wavelengths from 400 to 1100 nm, the optically active Tl, Pb and Bi centers in crystals have near-IR luminescence bands in a range of 1000–1700 nm.

Given that the near-IR bismuth luminescence bands in almost all of the bismuth-doped glasses studied to date are also located in this spectral region (Figures 1 and 2) and that Tl^0, Pb^{+} and Bi^{2+} are isoelectronic with each other ($6s^26p^1$), there is substantial reason to believe that the near-IR-emitting bismuth centers in glass are optical defect centers similar to the Tl, Pb and Bi centers in crystals. It is reasonable to assume that Bi-doped glass may contain the following optical defect centers: Bi^{2+} (1) (Bi^{2+} ion+an oxygen vacancy or another anion vacancy), Bi^{2+} (1)–Bi^{3+} dimer (Bi^{2+} and Bi^{3+} separated by a vacancy) and Bi^{+} (2) (a Bi^{+} ion between two vacancies). Given that the glass network has a disordered structure and contains a variety of defects, it seems likely that optical defect-emitting centers may contain not only anion vacancies, but also other defects of the glass network, which may modify the defect centers, causing a slight shift in the luminescence bands. Depending on the glass composition and the preparation conditions, only a portion of the above mentioned defect centers may form.

The following is experimental evidence of the proposed configurations of Bi-related near-IR-emitting centers:

- Near-IR luminescence has been observed in a Pb-doped germanosilicate fiber at 1100 nm.[23]
- Bi-, Pb-, Sn- and Sb-doped germanate glasses have similar near-IR luminescence spectra at various excitation wavelengths.[24] These experimental results and the isoelectronic structure of the Pb^{+}, Bi^{2+}, Sn^{+} and Sb^{2+} ions strongly suggest that these glasses contain similar near-IR-emitting centers.

It is clear that additional fundamental research on the nature of near-IR emission in Bi-doped glass is required.

NEAR-IR LUMINESCENCE PROPERTIES OF BI-DOPED OPTICAL FIBERS

The first Bi-doped optical fiber was fabricated in 2005 using the Modified Chemical Vapour Desposition (MCVD) technique.[25,26] The core of these fibers consisted of Bi-doped aluminosilicate glass. The creation of the first Bi-doped fiber laser was also demonstrated that year.[27]

Later, various types of Bi-doped optical fibers were developed, including fibers with cores consisting of Bi-doped SiO_2, Bi-doped GeO_2, Bi-doped P_2O_5–SiO_2, Bi-doped GeO_2–SiO_2 and Bi-doped P_2O_5–GeO_2–SiO_2 glass. The results of early investigations of the transmission and luminescence properties of various Bi-doped fibers are presented in a number of reviews and papers (see, for example Refs. 28–32).

The luminescence spectra of Bi-doped fibers were frequently obtained by excitation only at particular pumping wavelengths and *via* observation in a limited spectral region. Such measurements do not allow one to interpret the luminescence spectra correctly. Recently, we measured the luminescence intensity I_{lum} of Bi-doped fibers based on both emission and excitation wavelengths within a wide spectral range of 450–1700 nm. These measurements have allowed us to construct contour plots of the dependence I_{lum} (λ_{em}, λ_{ex}) for the following fibers: Bi–SiO_2, Bi–GeO_2, Bi–P_2O_5–SiO_2, Bi–Al_2O_3–SiO_2.[33]

Figure 3 shows the optical loss spectra of these Bi-doped fibers. All fibers have several broad absorption bands in visible and near-IR regions. The low curve corresponds to the aluminosilicate fiber, which is the first fiber fabricated and has well-known absorption bands at 500, 700, 800, 1000 and 1400 nm. In this figure, it is clear that the absorption spectra depend on the core glass composition. The fibers with silica and germanosilicate cores have similar absorption spectra.

Figure 4 shows the contour plots of the luminescence intensity for the fibers. The simplest luminescence picture is for the Bi-doped silica fiber (Figure 4a). The well-known red luminescence at 600 nm from Bi^{2+} is visible. A near-IR luminescence spectrum consists of two bands: one at 830 nm excited at 420 and 820 nm and one at 1430 nm excited at 420, 820 and 1420 nm. These bands will be further considered in relation to silica glass.

Figure 4b presents data for the Bi-doped germanate fiber. The first unexpected result is that there is no red luminescence from Bi^{2+}. Two new bands (in comparison with those of the Bi-doped silica fibers) appeared at 950 and 1650 nm. These bands will be further considered

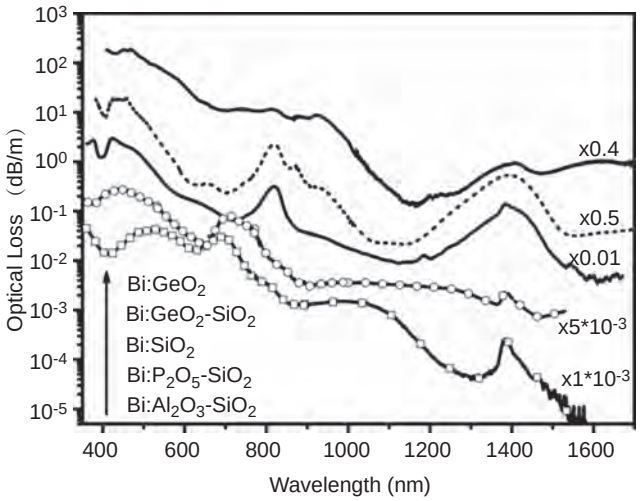

Figure 3 The optical loss spectra of Bi-doped germanate, germanosilicate, silica, phosphosilicate and aluminosilicate fibers.

in relation to germanate glass. The bands at 830 and ~1400 nm for silica glass are also observed. Their appearance can be explained by the diffusion of a small quantity of silicon from the silica cladding into the germanate core during the fiber fabrication.

Figure 4c shows the luminescence picture of the Bi-doped phosphosilicate fiber. The band at ~750 nm excited at 520 nm corresponds to Bi^{2+}. The bands at 830 and 1430 nm for silica are visible. There are broad luminescence bands in the spectral region of 1100–1300 nm for phosphorus.

The luminescence picture for the Bi-doped aluminosilicate fiber is presented in Figure 4d. The band at 750 nm corresponds to B^{2+}, the band at 820 nm to silica glass and the three broad bands in the spectral region of 1150–1300 nm to Al. It is interesting that there are no silica-related bands at 1400 nm, despite the significant amount of silica glass in the core of this fiber. This result can be explained as a function of the strong activity of Al in forming Al-Bi links. Given a limited concentration of Bi, practically all of the Bi ions are connected with Al, forming Bi–Al-emitting centers. However, if the Bi concentration increases (without an increase in the Al concentration), silica-related bands appear at 1400 nm.

Figure 5 summarizes the results presented. Taking into account the broad luminescence bands of the Bi-doped fibers (100 nm and more), one can see that the luminescence of the Bi-doped fibers extends from 800 to 1700 nm (through the whole spectral region). This figure also shows the lifetimes of the various luminescence bands. For the wavelengths longer than 1000 nm, the lifetime values are several hundred microseconds; for shorter wavelengths, they are 3–50 μs. A detailed discussion of the luminescence properties of Bi-doped fibers can be found in Ref. 33.

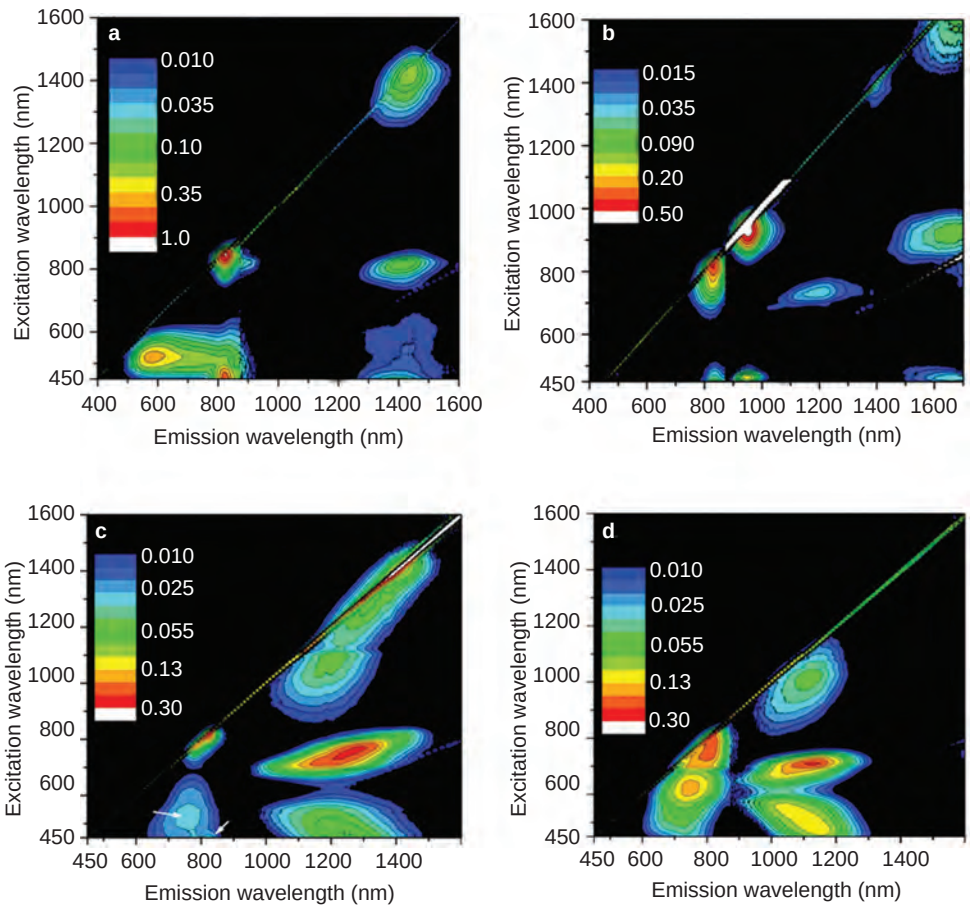

Figure 4 Contour plots of the luminescence intensity of Bi-doped SiO_2 (**a**), GeO_2 (**b**), P_2O_5–SiO_2 (**c**) and Al_2O_3–SiO_2 (**d**) fibers. The figures near colored stripes show relative intensities of the luminescence peaks.

doi:10.1038/lsa.2012.12

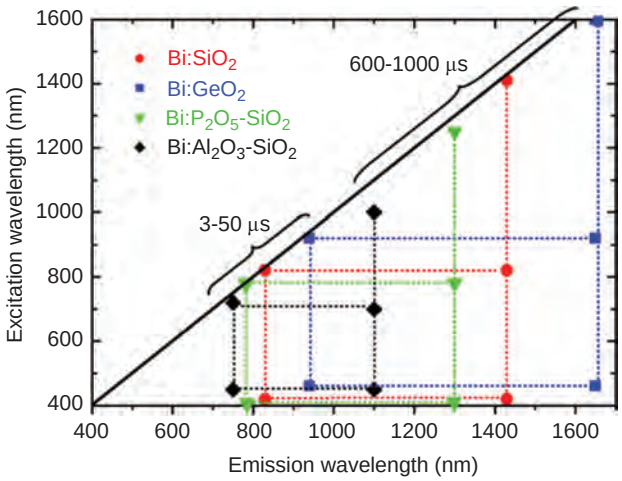

Figure 5 A summary scheme of the main emission peaks for different fibers. The types of fibers and lifetime values for various luminescence bands are also indicated.

BI-DOPED FIBER LASERS

The first Bi-doped fiber lasers were developed for a spectral region of 1140–1215 nm using Bi-doped aluminosilicate fibers. Later, Bi-doped fiber lasers were developed for a spectral region of 1270–1550 nm using newly developed phosphogermanosilicate, gremanosilicate and silica fibers. A review of the results of the efforts to develop the early Bi-doped fiber lasers is presented in Ref. 29.

Recently, high-power, efficient Bi-doped fiber lasers operating in a spectral region of 1390–1530 nm have been developed.[34–36] Bi-doped silica-based fibers codoped by Ge with a broad luminescence band at ~1400 nm were used as an active medium.

The laser operating at 1460 nm is presented in Figure 6. The length of the Bi-doped fiber was set at 95 m to provide nearly full absorption of the pump radiation at 1340 nm. A phosphosilicate fiber Raman laser was used as a pump source. The Raman laser was pumped by a Yb-doped fiber laser operating at 1137 nm.

Figure 7a shows the output power at 1460 nm as a function of pump power. The conversion efficiency of the laser was 50%. Figure 7b shows the dependence of the laser efficiency on temperature in comparison with that of Bi-doped fiber lasers based on phosphogermanosilicate and aluminosilicate fibers. Clearly, the efficiency of this laser depends only slightly on the temperature within a range of –60 to +80 ℃.

Figure 8 summarizes the results regarding the development of Bi-doped fiber lasers. The vertical axis shows the maximum output power of the continuous wave fiber lasers operating at corresponding wavelengths. The circles on the horizontal axis show the pumping wavelengths, with the color of the circles indicating the corresponding wavelengths generated. At present, the Bi-doped fiber lasers extend to the spectral region of 1140–1550 nm. However, given the wider spectral region associated with Bi-doped glasses and fibers, one might expect extension to shorter and longer wavelengths.

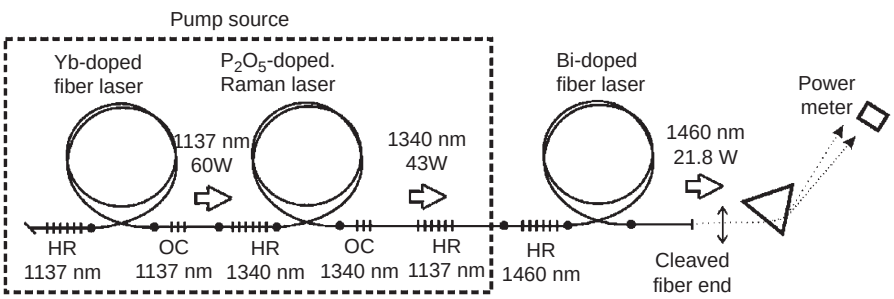

Figure 6 The 1460 nm Bi-doped fiber laser. HR, high reflectivity fiber Bragg grating; OC, output coupler.

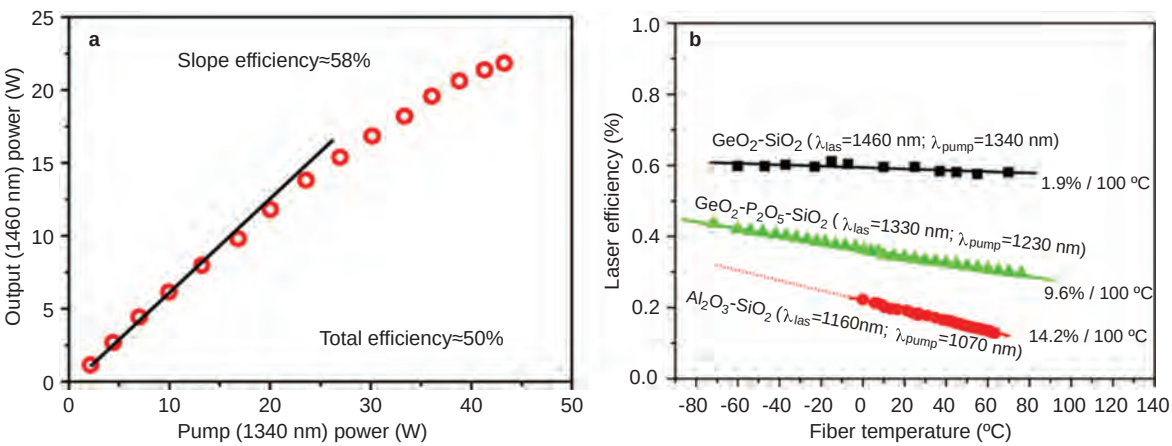

Figure 7 The dependence of output power on pump power (**a**) and the efficiency of various Bi-doped fiber lasers on temperature (**b**). λ_{las} and λ_{pump}, the wavelengths of laser generation and pump radiation respectively. On the right side of the picture "b" the laser efficiency changes (in %) per 100 ℃ temperature change are shown for fiber lasers with different core glass compositions.

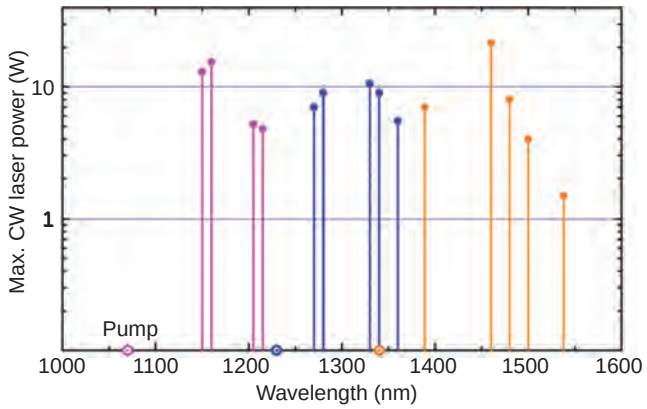

Figure 8 The output power of various Bi-doped fiber lasers operating in the spectral region of 1150–1550 nm. CW, continuous wave.

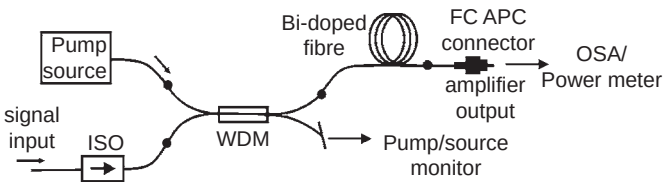

Figure 9 A Bi-doped fiber amplifier. ISO, optical isolator; WDM, wavelength division multiplexing coupler; OSA, optical spectrum analyzer; FC APC connector, Fiber-optics connector for Angled Physical Contact.

BI-DOPED FIBER AMPLIFIERS (BDFAs)

Optical amplifiers are the most essential element of modern optical fiber communication systems, continuously extending the reach of wavelength division multiplexing architectures. At present, commercial systems have a fiber transmission capacity of 10 Tbit s^{-1}. However, the global information demand increases by 30%–40% per year. Thus, in 20 years, the fiber transmission capacity will need to be 100–1000 Pbit s^{-1}. One of the ways to increase the fiber transmission capacity is to widen the transmission bands.

Today, high bit rate communication systems use a narrow spectral region of 1530–1610 nm for transmissions based on the amplification bandwidth of the Er-doped fiber amplifier. Granted, it is possible to use a spectral region of 1300–1500 nm, where the optical losses of silica-based fibers are less than 0.4 dB km^{-1}. However, there are no efficient optical amplifiers for this spectral region. Nevertheless, it follows from the results presented above that the development of Bi-doped fibers opens the door to the creation of an efficient BDFA for this spectral region.

The first results regarding the development of BDFA were obtained using a phosphogermanosilicate fiber.[37] Although we obtained a gain of more than 20 dB at 1320 and 1430 nm, the pumping power was notably high—460 and 190 mW, respectively.

Recently, a BDFA based on a Bi-doped germanosilicate fiber with improved characteristics and a commercial laser diode for pumping was developed.[38] The design of BDFA is presented in Figure 9.

The pump and the signal were launched through a wavelength division multiplexing coupler. The active fiber length was L=125 m. Two different pump sources were used:

1. a home-made Raman fiber laser with output power of up to 500 mW;
2. a commercially available, single-mode laser diode with output power of up to 80 mW at 1310 nm (LPSC-1310-FC; Thorlabs (Newton, New Jersey, USA)).

Two different kinds of light sources were used as signals:

1. a multiline signal source based on a supercontinuum fiber source and a set of high-reflectivity fiber Bragg grating (λ_s=1330–1650 nm, $\Delta\lambda_{FWHM}\approx$0.7 nm);
2. a fiber Bragg grating-stabilized diode laser at 1427 nm. We used an optical isolator (ISO in Figure 9) to suppress optical feedback and to prevent laser generation in the active fiber. The first signal source was used to measure the amplifier gain spectra and noise figure. The second source enabled us to examine the saturation characteristics of the amplifier.

Figure 10a shows the gain spectrum and the noise figure spectrum of the amplifier pumped by 65 mW at 1310 nm from a laser diode. The peak gain of 24-dB was observed near 1427 nm; the 3-dB bandwidth was 36 nm, and noise figure was 6 dB.

Figure 10b shows the gain at 1427 nm as a function of pump power at 1230 nm. The input signal power in this experiment was $P_{s_in}<-20$ dBm. The maximum gain coefficient (also called the pumping efficiency or gain efficiency) is G=0.4 dB mW^{-1}. The G value achieved is one order of magnitude lower than that of a typical Er-doped fiber amplifier but one order of magnitude higher than that of RFA and 2–4 times higher than that of Tm-doped fiber amplifiers. We expect that the appropriate optimization of the fiber parameters will allow us to increase the gain coefficient 2–4 times.

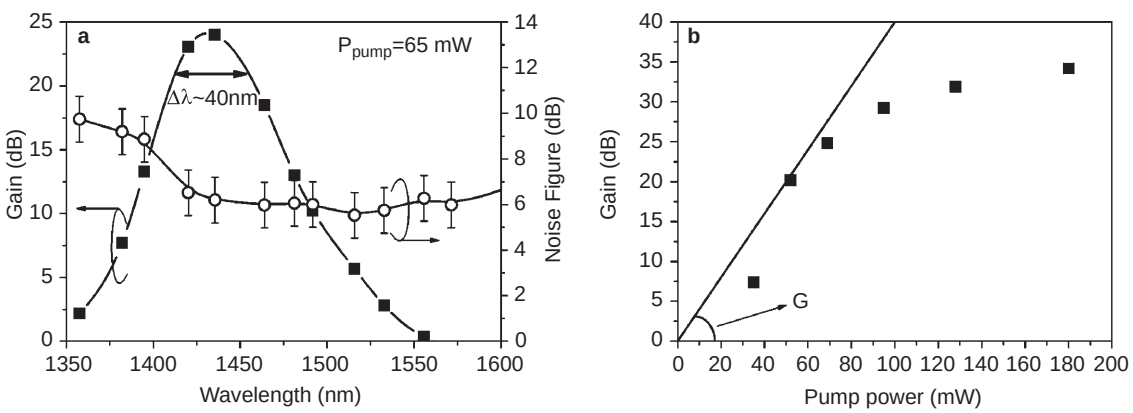

Figure 10 The gain and noise figure spectra of the amplifier (**a**) and dependence of gain on pump power at 1427 nm (**b**). G (dB mW^{-1}) is gain coefficient.

doi:10.1038/lsa.2012.12

CONCLUSION

Bismuth-doped fibers are a challenging active medium for near-IR lasers and optical amplifiers. Bi-doped fiber lasers and optical amplifiers in extended transmission bands have been demonstrated. However, the nature of Bi-related emission centers is not yet clear. Further fundamental research on the nature of Bi-emitting centers must be conducted to raise the efficiency of Bi-doped fiber lasers and optical amplifiers to the level exhibited by rare-earth-doped fiber devices.

ACKNOWLEDGMENTS

The author thanks Professor Bufetov and Dr Melkumov and Dr Firstov for their invaluable input on this paper.

1 Fujimoto Y, Nakatsuka M. Infrared luminescence from bismuth-doped silica glass. *Jpn J Appl Phys* 2001; **40**: L279–L281.
2 Dianov EM. Bi-doped glass optical fibers: is it a new breakthrough in laser materials? *J Non-Crystal Solids* 2009; **355**: 1861–1864.
3 Suzuki T, Ohishi Y. Ultrabroadband near-infrared emission from Bi-doped Li_2O–Al_2O_3–SiO_2 glass. *Appl Phys Lett* 2006; **88**: 191912-1–191912-3.
4 Hughes MA, Akada T, Suzuki T, Ohishi Y, Hewak DW. Ultrabroadband emission from a bismuth-doped chalcogenide glass. *Opt Express* 2009; **17**: 19345–19355.
5 Zhou Sh, Dong H, Zeng H, Feng G, Yang H *et al*. Broadband optical amplification in Bi-doped germanium silicate glass. *Appl Phys Lett* 2007; **91**: 061919-1–061919-3.
6 Douglas RW, Nath P, Paul A. Oxigen ion activity and its influence on the redox equilibrium in glasses. *Phys Chem Glasses* 1965; **6**: 216–223.
7 Corbett JD. Homopolyatomic ions of the post-transition elements–synthesis, structure and bonding. In: Lippard SJ, editor. Progress in Inorganic Chemistry, Vol. 21. John Wiley and Sons, Inc.; 1976; New York, London, Sydney, Toronto. pp129–158.
8 Khonton S, Morimoto Sh, Arai Y, Ohishi Y. Redox equilibrium and NIR luminescence of Bi_2O_3-containing glasses. *Opt Mater* 2009; **31**: 1262–1268.
9 Parke S, Webb RS. The optical properties of thallium, lead and bismuth in oxide glasses. *J Phys Chem Solids* 1973; **34**: 85–95.
10 Reisfeld R, Boehm L. Optical properties of bismuth in germanate, borax and phosphate glasses. *J Non-Crystalline Solids* 1974; **16**: 83–92.
11 Hamstra MA, Folkerts HF, Blasse G. Red bismuth emission in alkaline-earth-metal sulfates. *J Mater Chem* 1994; **4**: 1349–1350.
12 Srivastava AM. Luminescence of divalent Bismuth in M^{2+} BPO_5 ($M^{2+}=Ba^{2+}$, Sr^{2+} and Ca^{2+}). *J Lumin* 1998; **78**: 239–243.
13 Sanz O, Haro-Ponitovski E, Gonzalo J, Navarro JF. Influence of the melting conditions of heavy metal oxide glasses containing Bismuth oxide on their optical absorption. *J Non-Cryst Solids* 2006; **352**: 761–768.
14 Peng M, Dong G, Wondraczek L, Zhang L, Zhang N *et al*. Discussion on the origin of NIR emission from Bi-doped materials. *J Non-Cryst Solids* 2011; **357**: 2241–2245.
15 Dianov EM. On the nature of new IR emitting Bi centers in glass. *Quantum Electr* 2010; **40**: 283–285.
16 Goovaerts E, Andriessen J, Nistor SV, Schoemaker D. Electron-spin-resonance study of Tl atom defects in KCl and relativistic many-body analysis of the hyperfine structure. *Phys Rev B* 1981; **24**: 29–50.
17 Gelerman W, Luty F, Pollock CR. Optical properties and stable, broadlytunable CW laser operation of new F_A—type centers in Tl^+-doped alkali halides. *Opt Commun* 1981; **39**; 391–395.
18 Mollenauer LF, Vieira ND, Szeto L. Optical properties of the Tl^0 (1) center in KCl. *Phys Rev B* 1983; **27**: 5332–5346.
19 Ahlers FJ, Lohse F, Spaeth J-M. Identification of a Tl dimer centre in alkali halides by ODMR. *J Phys C: Sol State Phys* 1985; **18**: 3881–3890.
20 Fockele M, Lohse F, Spaeth J-M, Bartram RH. Identification and optical properties of axial lead centers in alkaline-earth fluorides. *J Phys: Condens Matter* 1989; **1**: 13–26.
21 Bartram RH, Fockele M, Lohse F, Spaeth J-M. Crystal-field model of the Pb^0 (2) centre in SrF_2. *J Phys: Condens Matter* 1989; **1**: 27–34.
22 Ruan J, Su L, Qiu J, Chen D, Xu J. Bi-doped BaF_2 crystal for broadband near-infrared light sourse. *Opt Express* 2009; **17**; 5163–5169.
23 Bufetov IA, Firstov SV, Khopin VF, Abramov AN, Guryanov AN *et al*. Luminescence and optical gain in Pb-doped silica-based optical fibers. *Opt Express* 2009; **17**: 13487–13492.
24 Sharonov M Yu, Bykov AB, Petricevich V, Alfano RR. Spectroscopic study of optical centers formed in Bi-, Pb-, Sb-, Sn-, Te- and In-doped germanate glasses. *Opt Lett* 2008; **33**: 2131–2133.
25 Dvoyrin VV, Mashinsky VM, Dianov EM, Umnikov AA, Yashkov MV *et al*. Absorption, fluorescence and optical amplification in MCVD Bismuth-doped silica glass optical fibers. Proceedings of European Conference on Optical Communication 2005, paper Th 3.3.5. September 25-29, 2005, Glasgo, published by the Institute of Electrical Engineers, London, GB.
26 Haruna T, Kakui M, Taru T, Ishikawa Sh, Onishi M. Silica-based Bismuth-doped fiber for ultra broad band light source and optical amplification around 1.1 μm. Proceedings of Optical Amplifiers and their Applications Topical Meeting 2005, paper MC3. 7-10 August 2005, Budapest, Optical Society of America, USA.
27 Dianov EM, Dvoyrin VV, Mashinsky VM, Umnikov AA, Yashkov MV *et al*. CW bismuth fiber laser. *Quantum Electr* 2005; **35**: 1083–1084.
28 Dianov EM. Bi-doped optical fibers: a new active medium for NIR lasers and amplifiers. *Proc SPIE* 2008; **6890**: 6890H-1–6890H-11.
29 Bufetov IA, Dianov EM. Bi-doped fiber lasers. *Laser Phys Lett* 2009; **6**: 487–504.
30 Razdobreev I, Bigot L, Pureur V, Favre A, Bouwmans G *et al*. Efficient all-fiber bismuth-doped laser. *Appl Phys Lett* 2007; **90**: 031103-1–031103-3.
31 Kalita MP, Yoo S, Sahu J. Bismuth-doped fiber laser and study of unsaturable loss and pump induced absorption in laser performance. *Opt Express* 2008; **16**: 21032–21038.
32 Truong VG, Bigot L, Lerouge A, Douay M, Razdobreev I. Study of thermal stability and luminescence quenching properties of bismuth-doped silicate glasses for fiber laser applications. *Appl Phys Lett* 2008; **92**: 041908-1–041908-3.
33 Firstov SV, Khopin VF, Bufetov IA, Firstova EG, Guryanov AN *et al*. Combined excitation-emission spectroscopy of bismuth active centers in optical fibers. *Opt Express* 2011; **19**: 19551–19561.
34 Firstov SV, Shubin AV, Khopin VF, Bufetov IA, Guryanov AN *et al*. The 20 W cw fiber laser at 1460 nm based on Si-associated bismuth active centers in germanosilicate fibers. CLEO/Europe – EQEC 2011, paper PDA. 7. 22-26 May 2011, Munich, Germany, Optical Society of America, USA.
35 Dianov EM, Bufetov IA, Firstov SV, Shubin AV, Medvedkov OI *et al*. Bismuth-doped silica-based fiber lasers operating near 1460 nm. Proceeding of European Conference on Optical Communication 2011, paper Tu 3 Le Cervin. 3. 18-22 September 2011, Geneva, Switzerland, Optical Society of America, USA.
36 Firstov SV, Shubin AV, Khopin VF, Melkumov MA, Bufetov IA *et al*. Bismuth-doped germanosilicate fiber laser with 20 W output power at 1460 nm. *Quantum Electr* 2011; **41**: 581–583.
37 Bufetov IA, Melkumov MA, Khopin VF, Firstov SV, Shubin AV *et al*. Efficient Bi-doped fiber lasers and amplifiers for the spectral region 1300–1500 nm. *Proc SPIE* 2010; **7580**: 758014-1–758014-9.
38 Melkumov MA, Bufetov IA, Shubin AV, Firstov SV, Khopin VF *et al*. LD pumped bismuth-doped optical fiber amplifier for 1430 nm band. *Opt Lett* 2011; **36**: 2408–2410.

This work is licensed under a Creative Commons Attribution-NonCommercial-NoDerivative Works 3.0 Unported License. To view a copy of this license, visit http://creativecommons.org/licenses/by-nc-nd/3.0